

Recent high-magnetic-field studies of unusual groundstates in quasi-two-dimensional crystalline organic metals and superconductors

J. Singleton, N. Harrison, R. McDonald, P.A. Goddard ^a
 A. Bangura, A. Coldea ^b L. K. Montgomery ^c X. Chi ^d

^a*National High Magnetic Field Laboratory, LANL, MS-E536, Los Alamos, New Mexico 87545, USA*

^b*Department of Physics, University of Oxford, Clarendon Laboratory, Parks Road, Oxford OX1 3PU, UK*

^c*Department of Chemistry, Indiana University, Bloomington, Indiana 47405, USA*

^d*Bell Laboratories, Lucent Technologies, 600 Mountain Avenue, Murray Hill, New Jersey 07974, USA*

Abstract

After a brief introduction to crystalline organic superconductors and metals, we shall describe two recently-observed exotic phases that occur only in high magnetic fields. The first involves measurements of the non-linear electrical resistance of single crystals of the charge-density-wave (CDW) system $(\text{Per})_2\text{Au}(\text{mnt})_2$ in static magnetic fields of up to 45 T and temperatures as low as 25 mK. The presence of a fully gapped CDW state with typical CDW electrodynamics at fields higher than the Pauli paramagnetic limit of 34 T suggests the existence of a modulated CDW phase analogous to the Fulde-Ferrell-Larkin-Ovchinnikov state. Secondly, measurements of the Hall potential of single crystals of $\alpha\text{-}(\text{BEDT-TTF})_2\text{KHg}(\text{SCN})_4$, made using a variant of the Corbino geometry in quasistatic magnetic fields, show persistent current effects that are similar to those observed in conventional superconductors. The longevity of the currents, large Hall angle, flux quantization and confinement of the reactive component of the Hall potential to the edge of the sample are all consistent with the realization of a new state of matter in CDW systems with significant orbital quantization effects in strong magnetic fields.

Key words: Organic metals, Superconductivity, Charge-density waves, High magnetic fields, Critical state phenomena, Fulde-Ferrell-Larkin-Ovchinnikov phase
PACS: 71.45.Lr, 71.18.+y, 71.20.Ps, 71.7.Di, 71.20.Rv

1 Introduction

Quasi-two-dimensional crystalline organic metals and superconductors are very flexible systems in the study of many-body effects and unusual mechanisms for superconductivity [1,2,3,4,5,6,7]. Their “soft” lattices enable one to use relatively low pressures to tune the same material through a variety of low-temperature groundstates, for example from Mott insulator via intermingled antiferromagnetic and superconducting states to unusual superconductor [4,6,7]. Pressure also provides a sensitive means of varying the electron-phonon and electron-electron interactions, allowing their influence on the superconducting groundstate to be mapped [3,4,8]. The self-organising tendencies of organic molecules means that organic metals and superconductors are often rather clean and well-ordered systems, enabling the Fermi-surface topology to be measured in very great detail using modest magnetic fields [3,9]; such information can then be used as input parameters for theoretical models [3]. And yet the same organic molecules can adopt a variety of configurations, leading to “glassy” structural transitions and mixed phases in otherwise very pure systems [4,10,11]; these states may be important precursors to the superconductivity in such cases [11].

Intriguingly, there seem to be at least two (or possibly three) distinct mechanisms for superconductivity [3,12,13,14] in the quasi-two-dimensional organic conductors. The first applies to half-filled-band layered charge-transfer salts, such as the κ -, β - and β' - packing arrangements of salts of the form $(BEDT-TTF)_2X$, where X is an anion molecule; the superconductivity appears to be mediated by electron correlations/ antiferromagnetic fluctuations [3,4,5]. The second mechanism applies to *e.g.* the β'' phase BEDT-TTF salts [4]; it appears to depend on the proximity of a metallic phase to charge order [11,12,13]. Finally, there may be some instances of BCS-like phonon-mediated superconductivity [14].

In addition to their invaluable role in mapping the bandstructure, high magnetic fields allow one to tune some of the organic conductors into some new and intriguing phases; examples include field-induced superconductivity [15] and exotic states such as the Fulde-Ferrell-Larkin-Ovchinnikov (FFLO) phase [16] (Fig. 1). In the remainder of this paper, we shall describe two recent observations of field-induced phases in crystalline organic metals, one of which is related to the FFLO but which results in an insulating state, and the other of which exhibits properties reminiscent of those of a superconductor, but via an entirely different mechanism.

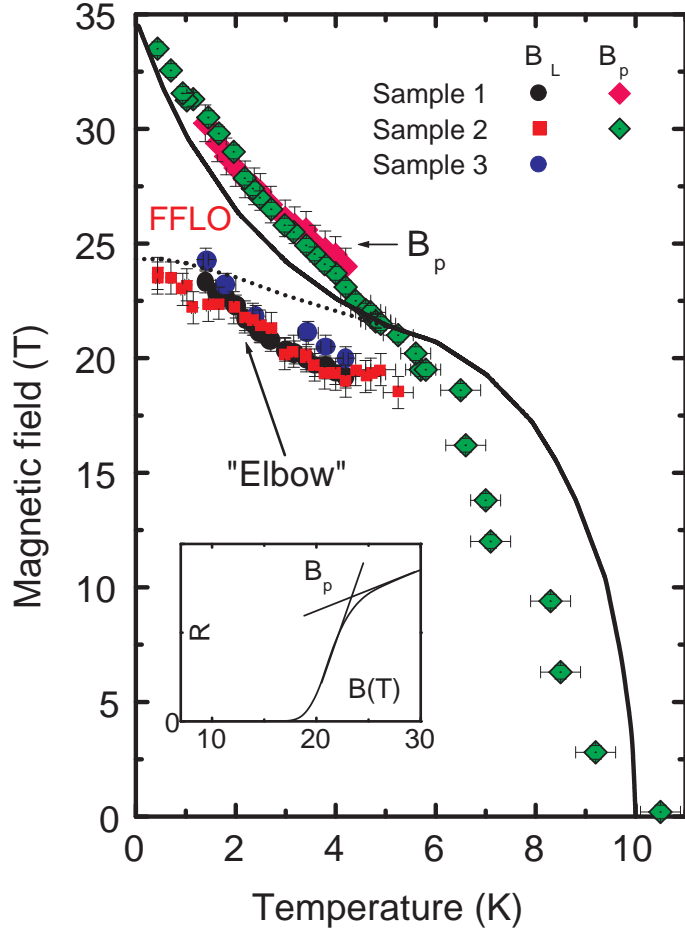


Fig. 1. Observation of the Fulde-Ferrell-Larkin-Ovchinnikov (FFLO) phase in κ -(BEDT-TTF)₂Cu(NCS)₂ [16]. The points labelled B_p denote the resistive upper critical field for two different samples (see inset for an illustrative example). The B_L points, denoting the phase boundary between the mixed phase and FFLO state were deduced using simultaneous MHz differential susceptibility measurements; the change in vortex stiffness that accompanies entry into the FFLO state causes an “elbow” in the field-dependent susceptibility. “Sample 3” is a measurement on a third sample under different conditions of electric field; consistency of the phase boundaries for the three samples shows that the effect is not due to artefacts of vortex pinning. The curves are a theoretical model due to Shimahara for the upper critical field and FFLO (see Ref. [16] for details).

2 Charge-density waves at fields above the Pauli paramagnetic limit

Intense magnetic fields (B) impose severe constraints on spin-singlet paired electron states. Superconductivity is one example of a groundstate where this is true, although orbital diamagnetic effects usually destroy superconductivity at lower magnetic fields than does spin-splitting [16,17]. Charge-density wave (CDW) systems, by comparison, are mostly free from orbital effects [18],

and so can only be destroyed by coupling B directly to the electron spin. While most CDW systems have gaps that are too large to be destroyed in laboratory-accessible fields [18], several new compounds have been identified within the last decade that have gaps ($2\Psi_0$) as low as a few meV, bringing them within range of the static magnetic fields at the National High Magnetic Field Laboratory.

As we shall discuss in Section 3, α -(BEDT-TTF)₂MHg(SCN)₄ (where $M = \text{K}$, Tl or Rb; $2\Psi_0 \sim 4$ meV) is one example that has been extensively studied [19]. However, it has a complicated phase diagram in a magnetic field owing to the imperfect nature of the nesting [20]; closed orbits exist after the Fermi-surface reconstruction which become subject to Landau quantization in a magnetic field [21], potentially modifying the groundstate. By contrast, (Per)₂M(mnt)₂ (where $M = \text{Pt}$ and Au) appears to be fully gapped [22]. However, the existence of spin $\frac{1}{2}$ moments on the Pt sites makes only the $M = \text{Au}$ system a pristine example of a small-gap, fully dielectric CDW material.

Measurements of the CDW transition temperature T_P (where the subscript “P” stands for “Peierls”) in (Per)₂Au(mnt)₂ ($T_P = 11$ K at $B = 0$) as a function of B indicate that it is suppressed in a predictable fashion [23], allowing a Pauli paramagnetic limit of $B_P \approx 37$ T to be inferred. However, the closure of the CDW gap with field is in fact considerably more subtle [24]; a finite transfer integral t_a perpendicular to the nesting vector produces a situation analogous to that in an indirect-gap semiconductor, where the minimum energy of the empty states above the chemical potential μ is displaced in k -space from the maximum-energy occupied states below μ [24]. Consequently, Landau quantization of the states above and below μ is possible, leading to a thermodynamic energy gap $E_g(B, T)$ of the form [24]

$$E_g(B, T) = 2\Psi(T) - 4t_a - g\mu_B B + \gamma\hbar\omega_c. \quad (1)$$

Here, $\Psi(T)$ is the temperature-dependent CDW order parameter ($\Psi(T) \rightarrow \Psi_0$ as $T \rightarrow 0$), ω_c is a characteristic cyclotron frequency in the limit $B \rightarrow 0$, and γ is a nonparabolicity factor; $g \approx 2$ is the Landé g-factor and μ_B is the Bohr magneton. Note that the Landau quantization *competes* with Zeeman splitting; however, at sufficiently high B it becomes impossible to sustain closed orbits, leading to a straightforward dominance of the Zeeman term [24].

Another subtlety in assessing the field-dependent thermodynamic gap (and hence the Pauli paramagnetic limit) in (Per)₂Au(mnt)₂ stems from the complicated nature of the low-temperature electrical conductivity, which contains contributions from both the sliding collective mode of the CDW and thermal excitation across the gap (see Fig. 2(a)) [24,25]. This leads to a measured resistivity $\rho_{yy} \approx (\sigma_T + j_y/E_t)^{-1}$, where σ_T is the conductivity due to thermal excitation across the gap and j_y/E_t is the contribution from the collective

mode, j_y being the current density and E_t the threshold field. Now Eq. 1 contains Ψ , which is T -dependent; moreover, E_t may also depend on T . Thus, Arrhenius plots are in general curved (see Fig. 2(b)), with a slope

$$\frac{\partial \ln \rho_{yy}}{\partial (1/T)} \approx \frac{\frac{1}{2k_B} (E_g - T \frac{\partial E_g}{\partial T}) - \frac{j_y T^2}{\sigma_T E_t^2} \frac{\partial E_t}{\partial T}}{1 + \frac{j_y}{\sigma_T E_t}}. \quad (2)$$

With appropriate choice of temperature and bias regimes, it is possible to make a reliable estimate of E_g from plots such as those in Fig. 2(b). On the other hand, it can be shown [26] that poorly-chosen experimental conditions (e.g. those of Ref. [23]) can easily lead to errors in the size of the derived gap.

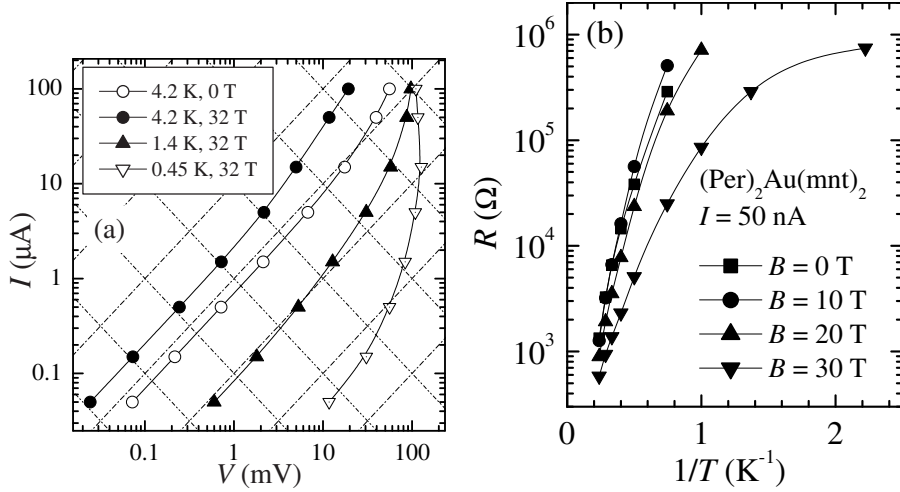


Fig. 2. (a) Non-linear current-versus-voltage characteristics of $(\text{Per})_2\text{Au}(\text{mnt})_2$ plotted on a logarithmic scale for various temperatures and fields (see inset key). The negative-slope diagonal lines are contours of constant power and the positive-slope diagonal lines are contours of constant resistance, providing a guide as to when the sample's behavior is dominated by ohmic, thermally-activated conduction rather than sliding. (b) Arrhenius plots of resistance R ($\propto \rho_{yy}$, logarithmic scale) versus $1/T$ with $I = 50 \text{ nA}$ for $(\text{Per})_2\text{Au}(\text{mnt})_2$ at several different B (after Ref. [24]).

Once accurate values of $E_g(B)$ have been obtained, the method of Ref. [24] can be used to fit Eq. 1 by adjusting the parameters $2\Psi_0 + 4t_a$, $4t_a$ and v_F , where v_F is the Fermi velocity in the metallic state; in the CDW state it is used to parameterise the quasiparticle dispersion. A good fit is obtained using $t_a = 0.20 \pm 0.01 \text{ meV}$, $v_F = (1.70 \pm 0.05) \times 10^5 \text{ ms}^{-1}$ and $2\Psi_0 = 4.02 \pm 0.04 \text{ meV}$ [24]. These parameters correspond to $E_g = 3.21 \pm 0.07 \text{ meV}$ at $B = 0$, $T = 0$; the derived transfer integrals t_a and t_b ($\approx 188 \text{ meV}$) are in good agreement with theory [27] and thermopower data [22]. (Note that these band parameters exclude the possibility of field-induced CDW (FICDW) states of the kind proposed in Ref. [28] in $(\text{Per})_2M(\text{mnt})_2$ salts.)

Armed with the band parameters, one obtains a reliable estimate of the Pauli paramagnetic limit; $B_P = (\Delta_0 + 2t_a)/\sqrt{2}gs\mu_B \approx 30$ T. This corresponds to a sharp drop in measured resistance R ($\propto \rho_{yy}$), as shown in Fig. 3 (left side), which displays data recorded at $T = 25$ mK. At such temperatures, there are very few thermally-activated quasiparticles indeed, leaving only the CDW collective mode to conduct; this gives rise to a R in Fig. 3 that is strongly dependent on current. On passing through $B_P \approx 30$ T, R drops very sharply, and there is also hysteresis between up- and down-sweeps of the field. The latter effect could be the consequence of a first-order phase transition on reaching B_P , compounded by CDW pinning effects.

However, the most interesting observation about Fig. 3 is the fact that the strongly non-linear $I - V$ characteristics persist at fields well above B_P , as can be seen from both R data and $I - V$ plots (right-hand side of Fig. 3). One can conclude from these data that it is only the threshold voltage for depinning the CDW that changes at B_P . This is probably a consequence of the CDW becoming incommensurate or of the order parameter of the charge modulation becoming considerably weakened [18,25]. Evidence for the latter is obtained by repeating the $I - V$ measurements at slightly higher temperatures of 900 mK (Fig. 3, right side). This temperature is sufficient to restore Ohmic behaviour for $B > B_P$, suggesting that a reduced gap for $B > B_P$ allows quasiparticles to be more easily excited.

There have been some interesting proposals for FICDW phases (e.g. Ref. [28]). These mechanisms would not cause the system to be completely gapped, but would instead lead to a closed orbit for one of the spins which would then have a Landau gap at the chemical potential. Such a situation leads to the quantum Hall effect, and a metallic behaviour of longitudinal resistivity [29]. Current would then be able to flow without the CDW having to be depinned. However, these effects are plainly absent from the data of Fig. 3; the continuation of the non-linear CDW electrodynamics for $B > B_P$ shows that metallic behaviour is not regained. Instead, both spin components of the Fermi surface are almost certainly gapped independently with differing nesting vectors, leading to an exotic CDW phase that has some analogies with the FFLO state of superconductors. The presence of two distinct, spin-polarized CDWs with different periodicities will furnish separate spin and charge modulations that could in principle be detected using a diffraction experiment [25].

3 A new quantum fluid in strong magnetic fields with orbital flux quantization

α -(BEDT-TTF)₂KHg(SCN)₄ is undoubtedly one of the most intriguing of BEDT-TTF-based charge-transfer salts [19,20,21]. Like many other such mate-

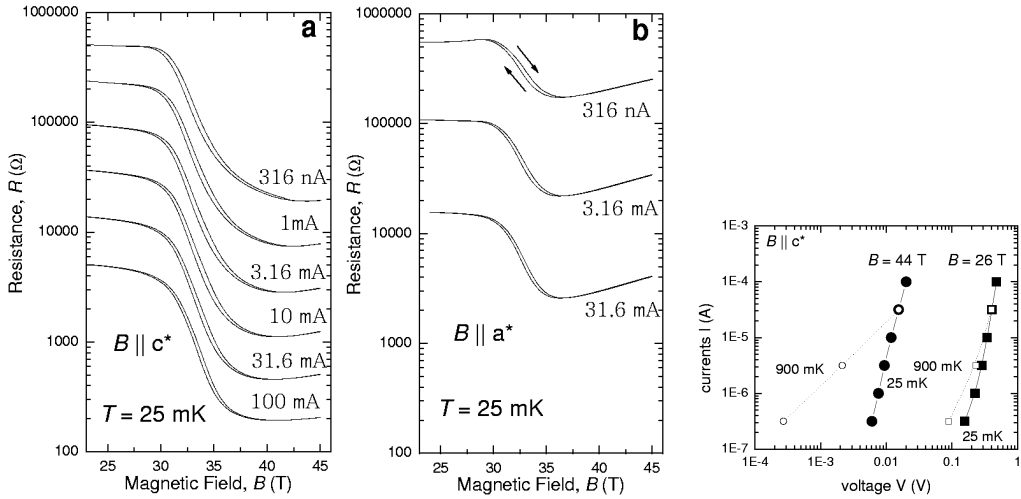


Fig. 3. Left: resistance of a single crystal of $(\text{Per})_2\text{Au}(\text{mnt})_2$ measured at 25 mK for fields between 23 and 45 T, for two different orientations c^* (a) and a^* (b) of B perpendicular to its long axis b , at several different applied currents. The lowest resistance for a given current occurs for B parallel to c^* , which is perpendicular to a^* . The dependence of the resistance on current signals non-ohmic behaviour. Right: non-linear current-versus-voltage characteristic of $(\text{Per})_2\text{Au}(\text{mnt})_2$ plotted on a log-log scale, for magnetic fields (26 and 44 T) above (circles) and below (squares) B_P . Filled symbols connected by solid lines represent data taken at 25 mK while open symbols connected by dotted lines represent data taken at 900 mK. (After Ref. [25].)

rials, it possesses both two-dimensional (2D) and one-dimensional (1D) Fermi-surface (FS) sections. However, the 1D sheets are unstable at low temperatures, causing a structural phase transformation below $T_P = 8$ K into a CDW state [30]. Imperfect nesting combined with the continued existence of the 2D hole FS pocket gives rise to complicated magnetoresistance and unusual quantum-oscillation spectra at low magnetic fields and low temperatures [14]. At high fields, the CDW undergoes a number of transformations into new phases, many of which have been suggested to be field-induced CDW phases [20].

Undoubtedly the most exotic aspect of this material is its transformation into a new state of matter above a characteristic field $B_k = 23$ T (known as the “kink” transition); B_k is now known to correspond to the CDW Pauli paramagnetic limit [21,14]. Such a regime is reached in α -(BEDT-TTF)₂KHg(SCN)₄ owing to the unusually low value of T_P [21]. At fields higher than B_k , Zeeman splitting of the energy bands makes a conventional CDW ground state energetically unfavourable [31], possibly yielding a novel modulated CDW state like that proposed for $(\text{Per})_2\text{Au}(\text{mnt})_2$ (see Section 2 and Refs. [24,25]). In α -(BEDT-TTF)₂KHg(SCN)₄ this state is especially unusual due to the existence of the 2D pocket, which appears to be ungapped by CDW formation [21]. The

CDW and 2D hole pocket screen each other, with pinning of the CDW then enabling a non-equilibrium distribution of orbital magnetization throughout the bulk [21]. Consequently, such a state exhibits a critical state analogous to that in type II superconductors, as shown in Fig. 4.

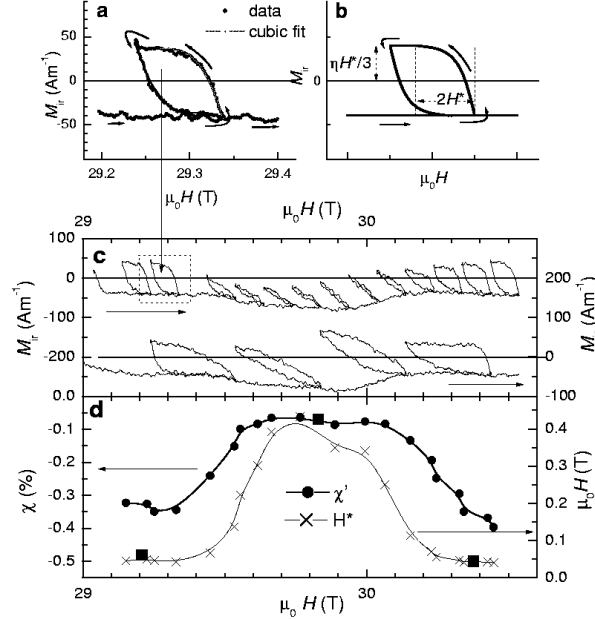


Fig. 4. Evidence for persistent currents and critical state behaviour in α -(BEDT-TTF)₂KHg(SCN)₄. (a) An example of a loop in the non-equilibrium component of the magnetization ΔM measured as the field is swept up to 29.33 T then momentarily down to 29.24 T before being resumed. Arrows indicate the change in the locus of ΔM versus H . The solid lines show the results of fits of ΔM to a Bean-type model of the critical state. (b) A model hysteresis loop calculated according to the Bean model for a long cylinder with its axis parallel to H , showing the theoretical saturation value of ΔM_z and the reversal state. (c) A series of ΔM versus H loops like that in (a) measured over an extended interval of field (top), and (bottom), a similar measurement but where the field interval over which the sweep direction is reversed is increased. Arrows indicate the appropriate axes. (d) Estimates of $\Delta\chi$ from fits of a Bean model to the many loops shown in (c) (full circles) Estimates of the coercion field H^* (x-symbols) are also shown. Arrows indicate the appropriate axes and square points are theoretical simulations. (After Ref. [21].)

This same non-equilibrium distribution also puts the CDW under considerable tension or compression, rather like a spring. Orbital quantization of the 2D pocket enables the magnetic field to be directly coupled to this “spring” via the variation of the chemical potential [21,32]. The magnetic field therefore provides a means to drive the compression and tension of the CDW and subsequent development of non-equilibrium persistent currents [21,32].

Attempts to drive a bulk current through α -(BEDT-TTF)₂KHg(SCN)₄ at low temperatures and $B > B_k$, either inductively or by way of external contacts,

causes the CDW to undergo compression or tension [21]. The build-up of potential energy in response to the current can be particularly strong at integral filling factors of the 2D pocket [21], giving rise to an effective force that is orthogonal to the current and the magnetic field and which varies approximately linearly across the width of the sample. Thus, there is a considerable energetic advantage in forcing the current towards the surface. Such a process protects the normal quasiparticles from inelastic scattering events, enabling the transport to become ballistic [21]. The electrodynamics of the 2D hole gas can then become significantly different than those of a regular dissipative material, allowing charge to accumulate inside the bulk that gives rise to an electric field orthogonal to the current j .

The electrodynamics can be summarized as follows [21]:

$$\frac{1}{2\omega_{c0}}\nabla^2V + \Delta B = 0; \quad (3)$$

$$\Delta B = -\frac{\mu_0\rho_{2D}}{B_0}V, \quad (4)$$

where V is the electrostatic potential, ΔB is the perturbation in background magnetic field B_0 due to a current, ω_{c0} is the unperturbed cyclotron frequency and ρ_{2D} is the charge density of the 2D pocket [21]. The first of these equations results from the effect of a charge build-up on the cyclotron motion and Landau level degeneracy whereas the second is simply the Hall effect in the absence of scattering. On combining these Equations, we obtain

$$\lambda^2\nabla^2V = V, \quad (5)$$

where $\lambda = (m^*/2\mu_0e\rho_{2D})^{1/2}$ is analogous to the London penetration depth in superconductors [21]; here m^* is the 2D quasiparticle effective mass. Eq. 5 describes an exponential screening of electric fields and currents from within the bulk [21]; it also suggests that an ideal Hall effect should occur in transport experiments, whereby a Hall angle $\Theta = \tan^{-1}(\rho_{xy}/\rho_{xx}) \rightarrow 90^\circ$ is observed.

Transport measurements made by applying contacts directly to samples of α -(BEDT-TTF)₂TlHg(SCN)₄ (which has the same groundstate as α -(BEDT-TTF)₂KHg(SCN)₄) have thus far proved inconclusive, owing mostly to the measured in-plane resistivity being contaminated by contributions from the interlayer component [33]. However, the Corbino geometry provides an alternative means of investigating the Hall voltage. In the case of α -(BEDT-TTF)₂KHg(SCN)₄, this is done according to the method of Ref. [34]. Because bulk single crystals of α -(BEDT-TTF)₂KHg(SCN)₄ cannot be easily machined into arbitrary shapes, contacts must be placed between the geometric center of the circulating current path and the sample edge [21,34].

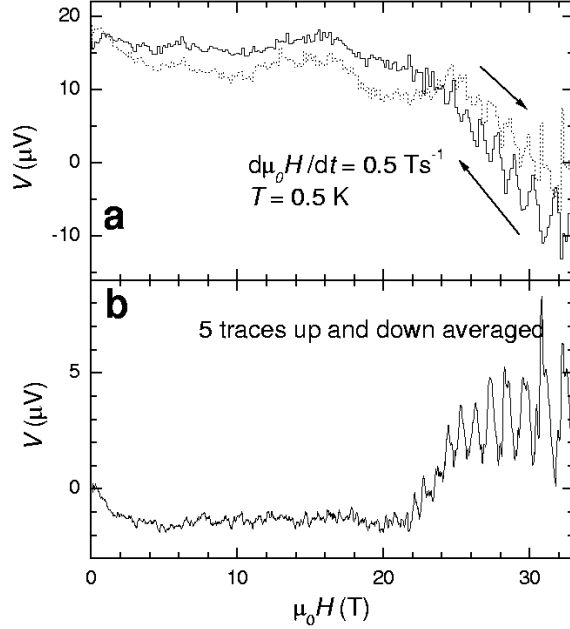


Fig. 5. An example of the Hall potential V_H of a α -(BEDT-TTF)₂KHg(SCN)₄ sample in a slowly varying magnetic field (sweep rate $\partial\mu_0 H/\partial t = 0.5 \text{ T}^{-1}$; $T = 0.50 \text{ K}$). (a) shows raw data for a single sweep, with arrows indicating the sweep direction. No filtering has been applied. The background non oscillatory component could be caused by variations in the contact potentials with magnetic field. (b) The difference $(V_{H,\text{up}} - V_{H,\text{down}})/2$ between rising- and falling-magnetic-field data averaged over 5 sweeps. (After Ref. [21].)

This experimental scheme constitutes perhaps the simplest possible measurement that can be made in a magnetic field [21]. The two contacts are connected directly to the input of a voltmeter that detects the induced voltage as the field is slowly swept. Data are shown in Fig. 5, in which the Hall voltage is given by

$$V_H = \frac{A\mu_0}{4\pi} \frac{\partial H}{\partial t} \tan \Theta, \quad (6)$$

where $A \approx 1 \text{ mm}^2$ is the cross-section of the sample. Eq. 6 implies that $\Theta = 89.7^\circ$ at the highest fields, which is perhaps the highest value ever reported for a single-crystal sample. The greatest sensitivity is, however, obtained by using a small sinusoidal ac magnetic field superimposed on top of the background field, which enables the normal (i.e. in phase with the voltage induced in a conventional coil) and reactive components to be extracted [21]. A reactive Hall voltage component V_H'' indicates the existence of long-lived free currents, and is only observed at fields $B > B_k$ (Fig 6); this is expected by virtue of the fact that this new state of matter only exists in the high-magnetic-field regime.

If the reactive current is confined mostly within a distance λ of the sample edge, the Hall voltage drop should also occur mostly within that distance [21]. Fig. 6 shows that the reactive Hall voltage drop occurs within a distance that is too small to be detected using regular contacts applied using graphite paint. The normal component is also unusual, but shows a weak penetration of the normal in-phase Hall electric field into the bulk.

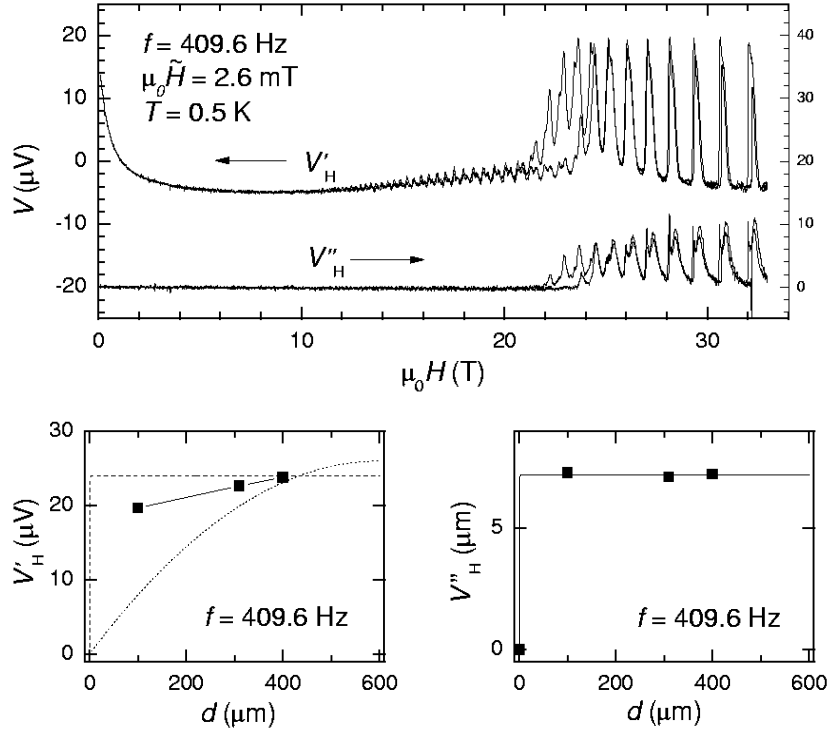


Fig. 6. Top: examples of the in-phase and quadrature Hall potentials V'_H and V''_H in α -(BEDT-TTF)₂KHg(SCN)₄. An oscillatory applied field with $\mu_0 \tilde{H} \approx 2.6$ mT rms and $\omega/2\pi = 409.6$ Hz was used; $T \sim 0.5$ K. Arrows indicate the axis corresponding to each data set. Bottom: the Hall potential difference between the edge and a voltage probe situated a distance d inside the upper surface where $d = 100, 310$ and 400 μm with $T = 0.5$ K, $f = 409.6$ Hz and $\mu_0 \tilde{H} = 2.6$ mT. (a) shows the normal Hall voltage V'_H . The dotted line shows the voltage distribution expected with a very high conventional conductivity while the dashed line shows the voltage distribution expected for an exponential variation of the Hall potential, $V_H \propto \exp(-d/\lambda)$. (b) shows the reactive Hall voltage V''_H , with the solid line depicting $V_H \propto \exp(-d/\lambda)$ with $\lambda \ll 100$ μm . (After Ref. [21].)

In summary, measurements of the Hall potential difference on single crystals of α -(BEDT-TTF)₂KHg(SCN)₄ provide compelling evidence for this existence of a new type of quantum fluid resulting from the mutual coupling of a 2D hole gas to a gapped CDW system [21]. Such a large reactive Hall potential difference is not observed in conventional metals. In this quantum fluid, the build up of charge in the bulk within a distance λ of the surface prevents the

CDW from having to be coerced by a changing magnetic field into a non-equilibrium state, thereby conserving energy.

Finally, it should be noted that an analysis of the ratio of magnetic flux saved per 2π phason of the CDW (via trivial algebraic manipulation of the results of Ref. [21]) reveals an unusual virtual quantization of magnetic flux per phason of the form

$$\Phi_0 = \frac{h}{2\nu e}, \quad (7)$$

where ν is the Landau-level filling factor of the 2D hole system at integral Landau-level filling factors. The flux quantization is irrational at other filling factors.

Acknowledgements

This work is funded by US Department of Energy (DoE) grant LDRD 20040326ER. Work at NHMFL is performed under the auspices of the National Science Foundation, DoE and the State of Florida.

References

- [1] B.J. Powell and R.H. McKenzie, *J. Phys.: Condens. Matter* 16, L367 (2004).
- [2] M.T. Dressel and N. Drichko, *Chemical Reviews*, 104, 5689 (2004).
- [3] J. Singleton and C.H. Mielke, *Contemp Phys.* 43, 63 (2002).
- [4] B.J. Powell and R.H. McKenzie, *Phys. Rev. Lett.* 94, 047004 (2005).
- [5] B.J. Powell and R.H. McKenzie, *Phys. Rev. B* 69, 024519 (2004).
- [6] F. Kagawa et al., *Phys. Rev. Lett.* 93, 127001 (2004).
- [7] S. Lefebvre et al., *Phys. Rev. Lett.* 85, 5420 (2000)
- [8] R.D. McDonald et al., *J. Phys.: Condens Matter* 15, 5315 (2003).
- [9] P.A. Goddard et al., *Phys. Rev. B* 69, 174509 (2004).
- [10] J. Singleton et al., *J. Phys.: Condens. Matter* 15, L203 (2003)
- [11] A.I. Coldea et al., *Phys. Rev. B* 69, 085112 (2004)
- [12] J. Merino and R.H. McKenzie, *Phys. Rev. Lett.* 87, 237002 (2001).

- [13] P.A. Goddard et al., *J. Phys.: Condens. Matter* 14, 7345 (2002).
- [14] J. Singleton, *Rep. Prog. Phys.* 63, 1111 (2000).
- [15] S. Uji et al., *Nature* 410, 908 (2001).
- [16] J. Singleton et al., *J. Phys.: Condens. Matter* 12, L641 (2000).
- [17] M. Tinkham, *Introduction to Superconductivity* (McGraw-Hill, 1994).
- [18] G. Grüner, *Density waves in solids*, *Frontiers in physics* 89 (Addison-Wesley, 1996).
- [19] N. Harrison et al., *Phys. Rev. B* 62, 14212 (2000).
- [20] D. Andres et al., *Phys. Rev. B* 68, 201101 (2003).
- [21] N. Harrison et al., *Phys. Rev. B* 69, 165103 (2004).
- [22] M. Matos et al., *Phys. Rev. B* 54, 15307 (1996).
- [23] D. Graf et al., *Phys. Rev. B* 69, 125113 (2004).
- [24] R. McDonald et al., *Phys. Rev. Lett.* 94, 106404 (2005).
- [25] R. McDonald et al., *Phys. Rev. Lett.* 93, 076405 (2004).
- [26] R.D. McDonald et al., *cond-mat* 0408408 (2004).
- [27] R.T. Henriques, *J. Phys. C* 17, 5197 (1984).
- [28] D. Graf et al., *Phys. Rev. Lett.* 93, 076406 (2004).
- [29] P. M. Chaikin, *J. Phys. I (France)* 6, 1875 (1996).
- [30] P. Foury-Leykleian et al., *Synth. Met.* 137, 1271 (2003).
- [31] R. H. McKenzie, *cond-mat/970635*.
- [32] N. Harrison, *Phys. Rev. B* 66, 121101(R) (2002).
- [33] N. Harrison et al., *Phys. Rev. B* 55, 16005 (1997).
- [34] M. M. Honold et al., *Phys. Rev. B* 59, R10417 (1999).